https://dx.doi.org/10.21577/0103-5053.20200075

J. Braz. Chem. Soc., Vol. 31, No. 9, 1859-1872, 2020
Printed in Brazil - ©2020 Sociedade Brasileira de Química

Article

Accessing Basic Sites on Modified $CoFe_2O_4$ Nanoparticles: Addressing the Selective Oxidation of Benzyl Alcohol and Unraveling the Au:Pd Ratio Effects by XPS

Laíse N. S. Pereira,[a,b] Marco A. S. Garcia,[c,d] Jennifer Rozendo,[d] Pedro Vidinha,[d] Alfredo Duarte,[d] Carla V. R. de Moura[a] and Edmilson M. de Moura[*,a]*

[a]*Departamento de Química, Universidade Federal do Piauí, Campo Universitário Ministro Petrônio Portela, Bairro Ininga, 64049-550 Teresina-PI, Brazil*

[b]*Instituto Federal do Maranhão, Campus São Raimundo das Mangabeiras, Rodovia BR-230, km 319, 65840-000 São Raimundo das Mangabeiras-MA, Brazil*

[c]*Departamento de Química, Universidade Federal do Maranhão, Avenida dos Portugueses, 1966, 65080-805 São Luís-MA, Brazil*

[d]*Departamento de Química Fundamental, Instituto de Química, Universidade de São Paulo, Avenida Professor Lineu Prestes, 748, 05508-000 São Paulo-SP, Brazil*

AuPd nanoparticles have gained substantial attention due to their application in selective oxidation of alcohols. However, due to the radical nature of the oxidation of benzyl alcohol, under specific conditions, even without a catalyst, the reaction occurs and affects the selectivity of the system. Therefore, we aimed to develop a catalyst that enables the control of the oxidation leading to higher reaction selectivity. To accomplish this, we have prepared a catalytic support comprised of $CoFe_2O_4$ nanoparticles impregnated with $Sr(OH)_2$ that presented a significant control of the reaction selectivity without any metal or external base addition. After the impregnation of AuPd nanoparticles in a specific ratio, the reaction reached a selectivity of > 99% for benzaldehyde, in 3.5 h, with a recycle regime of five runs without loss of activity and selectivity. Our results show that the judicious choice of the ratio of the metals prevents the necessity of manipulating the reaction conditions to improve the performance of the system. Additionally, studies under N_2 and O_2 environments, with or without water, confirmed the role of the O_2 in the system. Holding all this information, we propose a possible mechanism for the prepared system.

Keywords: $Sr(OH)_2$, AuPd nanoparticles, oxidation, mechanism

Introduction

The selective oxidation of alcohols to their respective aldehydes, esters, carboxylic acids, or ketones is a versatile functional-group transformation pursued by both academia and industry.[1-4] They are key intermediates for the synthesis of fine chemicals, fragrances, medicines, and other chemical transformations.[5] The design of easy to recover heterogeneous catalysts that avoid the overoxidation is of great importance as the use of stoichiometric chromium and manganese-based reagents[6,7] is still very common. As an alternative, gold catalysts have been intensively studied for alcohol oxidations since the seminal work of Prati and co-workers.[8-10] However, gold leads to low activity without the promotion of external bases,[11] basic oxide supports,[12] or the addition of a second metal,[13] being the last two the most promising approaches for obtaining high-performance catalysts.

Platinum group metals are much more active than gold towards hydrogen abstraction.[14] When palladium is used as active species in association with gold nanoparticles (NPs), enhanced performances are observed when comparing them with the monometallic counterparts.[15] Their remarkable synergy tends to prevent overoxidation and poisoning with an optimized chemical composition.[16,17] The role of AuPd synergistic effects is usually attributed to electronic and geometric effects. However, maintaining a sharp size distribution of bimetallic NPs by choosing an appropriate synthesis approach, electronic issues are more easily studied. Once Au presents the highest electronegativity among the transition metals, AuPd-based bimetallic catalysts tend to have electron transfer from the Pd to Au,[18]

*e-mail: mmoura@ufpi.edu.br

which affects the catalytic performance of the system by electronic issues. These modifications can be achieved by regulating the surface composition of the bimetallic structures by varying their AuPd ratios,[19] which could provide tunable catalytic performances.

After the metal composition, the choice of catalytic supports is not a straightforward task, which reveals the need to prepare specific catalysts that take into consideration the reaction type, active species, and support interaction/functionality.[20] Corma and Iborra[21] have discussed the apparent lack in the fundamental knowledge of catalysis and the industrial application of basic materials. The general strength of basic sites,[22] BaO > SrO > CaO > MgO, and the strength of oxygen Lewis basic sites on alkaline earth metal oxides,[21] O_2 > OH > H_2O > H_3O^+, both suggest the use of $Sr(OH)_2$ as a suitable material for catalytic support towards oxidations. Nevertheless, its use for this particular application is still neglected in the literature. Also, the possibility of associating this compound with a magnetic carrier is stimulating since this separation tool would be easily used in the industry under electromagnetic fields.[23] Using a suitable approach, mechanism insights are possible to be proposed, associating careful experimental data and characterization techniques.

In addition to the careful selection of the metal ratios and support, the chosen substrate can be used to help to rationalize the specificities that a novel catalytic system possesses. The oxidation of benzyl alcohol under certain conditions, without the addition of a catalyst, has not been comprehensively studied. Such process affects the selectivity of the system;[24] thus, it is mandatory to design catalysts that guarantee the controlling of the overall reaction. Sankar *et al.*[25] have studied the autoxidation of benzaldehyde, and have proposed that the benzyl alcohol itself controls the reaction since it quenches the oxidation process by intercepting acyl peroxy radicals. However, the oxidation of benzyl alcohol under certain conditions, without active species, and how the catalyst acts in its controlling have not been considered.

Herein, we present the synthesis of a strontium hydroxide-modified $CoFe_2O_4$ support, which presented substantial influence in the adjusting of benzyl alcohol oxidation. Also, after the immobilization of a specific Au:Pd ratio, the catalyst presented a superior improvement on the controlling of the oxidation products, affording > 99% of selectivity for the partially oxidized product in 3.5 h. Using X-ray photoemission spectroscopy (XPS), transmission electron microscopy (TEM), and scanning transmission electron microscopy (STEM) with energy dispersive spectrometer (EDS), in association with time online profiles of different Au:Pd ratios immobilized on the support, addition of water, and controlled gaseous environment, we have rationalized the synergy of the Au:Pd ratio and proposed a mechanism for the system.

Experimental

All chemicals were of analytical grade, bought from Sigma-Aldrich (São Paulo, Brazil) or Vetec (São Paulo, Brazil), and used as received, without further purification or treatment, except when mentioned ahead. All solutions were prepared using deionized water (18.2 MΩ cm, SPLabor, São Paulo, Brazil).

Synthesis of the $CoFe_2O_4$ NPs and $Sr(OH)_2/CoFe_2O_4$ support

Cobalt ferrite NPs were prepared by using a co-precipitation method.[26] In a typical synthesis, 2.5 mL of an aqueous acid solution (2 mol L^{-1} HCl) of $CoCl_2.6H_2O$ (4.1 mmol) was added to 5 mL of an aqueous solution of $FeCl_3.6H_2O$ (8.2 mmol). Then, the resulting solution was added to 125 mL of an aqueous ammonium hydroxide solution (0.7 mol L^{-1}) under vigorous stirring (900 rpm, Arec X, Velp Scientifica). Instantly, the formation of a black precipitate was observed. After additional stirring (2 h) at the same rotation, the solid was collected with a $Nd_2Fe_{14}B$ (neodymium) magnet, and the supernatant poured off. The black solid was washed several times with hot water (200 mL, 80 °C) to eliminate ammonium ions, once with acetone (100 mL), and dried at 80 °C in an oven. After 12 h of drying, the material was calcined in the air at 800 °C for 3 h, at a heating rate of 10 °C min^{-1}.

Commercial strontium carbonate was calcined at 1100 °C for 5 h in air atmosphere. The as-prepared SrO was used for modifying the $CoFe_2O_4$ NPs surface by an impregnation method.[27] The materials were mixed in acetone under vigorous stirring (1000 rpm) for 24 h. The mass of SrO was five times the mass of the $CoFe_2O_4$ NPs. After this time, the material was dried in an oven at 100 °C for 12 h. Rietveld refinement presented in the Results and Discussion section showed that the strontium compound was comprised of a mixture of different phases of $Sr(OH)_2$, this is the reason for the designation of $Sr(OH)_2/CoFe_2O_4$ for the support synthesized.

Preparation of Au, Pd, and Au-Pd catalysts (monometallic catalysts)

The catalysts were prepared using a sol-immobilization method with modifications.[28]

$Au/Sr(OH)_2/CoFe_2O_4$ catalyst

For the controlling of NPs growth, 1.80 mL of an aqueous polyvinyl alcohol solution (PVA 80%; 2.0 wt.%; 36 mg) was poured into an aqueous solution of gold(III) chloride trihydrate ($HAuCl_4$, 30 wt.% in dilute HCl; 172.5 mg; 300 mL) under vigorous magnetic stirring (900 rpm). To promote the reduction of the metal, a recently prepared aqueous solution of sodium borohydride ($NaBH_4$; 0.1 mol L^{-1}; 7.65 mL) was added to the mixture under magnetic stirring. The solution instantly turned darkish. After 30 min of stirring, the support was added (1.5 g) to the solution and stirred at room temperature for 3 h. The catalyst was recovered using a neodymium magnet and washed three times with hot water (100 mL, 80 °C) and once with acetone (100 mL) before drying at 80 °C for 12 h.

$Pd/Sr(OH)_2/CoFe_2O_4$ catalyst

The same procedure described before was used for the Pd-comprised catalyst, except for the metal precursor: palladium(II) chloride ($PdCl_2$) in 10 wt.% HCl to make up to 2% of Pd loading over the support.

$AuPd/Sr(OH)_2/CoFe_2O_4$ catalysts

Three Au:Pd ratios were used for the catalysts syntheses: Au:Pd 1:1, Au:Pd 1:1.5, and Au:Pd 1:2. As an example, the Au:Pd 1:1.5 NPs synthesis is described.

An aqueous solution containing 8.6 mg of $PdCl_2$ in 10 wt.% HCl was added in 30 mL of an aqueous solution containing 27.6 mg of $HAuCl_4$. After 5 min of vigorous magnetic stirring (9000 rpm) at room temperature, 0.6 mL of a 2.0 wt.% aqueous solution of PVA was added to the solution. Successively, a freshly prepared aqueous solution of 0.1% of $NaBH_4$ was added under magnetic stirring, and the solution turned darkish instantly. After 30 min of stirring, 500 mg of the support was added to the sol prepared and stirred for 2 h, at room temperature. The catalyst was separated using a neodymium magnet and was dried in an oven at 80 °C for 12 h.

Catalytic reactions

The reactions were performed in a Fischer-Porter glass reactor of 100 mL at 2 bar of O_2 and 100 °C, except when mentioned. The catalyst (4.1 μmol of metal) and benzyl alcohol (1 mL, 9.6 mmol) were added into the reactor and stirred for a specific time, which was specified ahead. At the ending of the reaction, the catalyst was recovered using a neodymium magnet by placing it on the reactor wall. For analytical analyses, 10 μL of the final solution was collected and added to 1 mL of CH_2Cl_2. The injection in the gas chromatograph was performed by using 1 μL of the prepared solution. In the recycling experiments, the catalyst was washed with 3 mL of CH_2Cl_2, dried in an oven for 1 h at 80 °C and reused. The tests with N_2 were carried out under the same reaction conditions of the tests with O_2. To evaluate the effect of water in the oxidation reaction, 0.5 mL of water was added to 1 mL of benzyl alcohol at the beginning of the reaction.

The conversion, selectivity, and carbon mass balance of benzyl alcohol were calculated as follows:

$$\text{Conversion}(\%) = \frac{\text{Alcohol}_{\text{begin,mol}} - \text{Alcohol}_{\text{after,mol}}}{\text{Alcohol}_{\text{begin,mol}}} \times 100 \quad (1)$$

$$\text{Selectivity}(\%) = \frac{\text{Product of interest}_{\text{mol}}}{\text{All products}_{\text{mol}}} \times 100 \quad (2)$$

$$\text{Carbon mass balance}(\%) = \frac{\text{Total moles of products and unreacted substrate}}{\text{Initial moles of substrate}} \times 100 \quad (3)$$

The carbon mass balance in the performed experiments was always higher than 95%.

Characterizations

X-ray diffraction (XRD) analyses were performed using a Bruker D8 Advance equipment (Bruker AXS GmbH, Karlsruhe, Germany) with Cu Kα radiation and a graphite monochromator. The scans were recorded in the 2θ range between 10 and 90° using a step size of 1°. The phase composition was determined by Rietveld refinement using ReX software version 0.8.2.[29] The XPS spectra were obtained with a Scienta Omicron ESCA + spectrometer system equipped with an EA 125 hemispherical analyzer and an XM 1000 monochromated X-ray source (Scientia Omicron, Uppsala, Sweden) in Al Kα (1486.7 eV). The analyses were performed by using CasaXPS processing software version 2.3.15.[30] Surface parameters of the catalysts were determined from nitrogen adsorption isotherms, recorded at −196 °C in an Autosorb IQ-Quantachrome Instrument (Florida, USA). Specific surface areas were determined by Brunauer-Emmett-Teller (BET) method in a relative pressure range of $0.07 < P/Po < 0.3$; Barrett-Joyner-Halenda (BJH) method was used to determine the average pore diameter. The STEM images of the materials were obtained with an FEI Tecnai G2 F20 transmission electron microscope (Thermo Fisher Scientific, Massachusetts, USA) with an energy dispersive spectrometer (Bruker XFlash 6130T Silicon Drift Detector, USA). The element distribution maps were recorded using energy-dispersive X-ray spectrometry (EDS). TEM images were obtained using a JEOL JEM 2100 microscope (JEOL,

Tokyo, Japan). The nanoparticles' sizes were determined by using the image processing program ImageJ.[31] For that, 300 particles were considered. Samples for microscopy were prepared by drop-casting an isopropanol suspension of the materials over a grid comprised of carbon-coated copper, followed by drying under ambient conditions. Metal loading and leaching analyses were performed using a Shimadzu GFA-EX7i (Kyoto, Japan) flame atomic absorption spectrometer (FAAS) equipped with a pneumatic nebulizer system.

Results and Discussion

Support synthesis and characterization

Recently, the promotion of strontium compounds as suitable catalytic supports for alcohol oxidation reactions has been studied.[32-35] We have proposed that the intrinsic basicity of strontium compounds is an important issue for promoting the reaction, considering that the support can be directly related to the catalytic cycle mechanism. Thus, the improvement of strontium-based supports and their correlation with the performance of the catalyst is highly desired.

The aim here is to step forward into the knowledge of the support effect on the catalysis progress, give insights related to the reaction mechanism, and obtain a catalyst easy to recover from the reaction medium. Therefore, by using a simple co-precipitation method, we prepared a magnetic material able to afford interaction with strontium hydroxide (prepared by calcination of $SrCO_3$ at 1100 °C). Such a procedure envisaged the possibility of using the $CoFe_2O_4$ as a separation tool once without the modification it was not applicable for PVA-stabilized NPs immobilization,[28] due to its low interaction with the NPs. Also, the procedure aimed to explore the alkaline properties of the strontium compound prepared, which the specific crystalline phases were clarified herein.

The composition of the as-prepared $CoFe_2O_4$ NPs was analyzed by Rietveld refinement to specify the number and amount of crystalline phases. As observed in Figure 1a, the material seems to present a single phase, which is important to guarantee that the interaction between the $CoFe_2O_4$ NPs and the strontium compound is the same in all the extension of the material. The diffraction pattern indexed one phase: cubic $CoFe_2O_4$ (Inorganic Crystal Structure Database (ICSD) 109045). After the impregnation of the $CoFe_2O_4$ NPs, another Rietveld refinement was performed to elucidate the strontium phases, as well as any changes in the $CoFe_2O_4$ phase. Figure 1b shows the pattern of the material, with three indexed phases: $CoFe_2O_4$ (ICSD 109045), $Sr(OH)_2$ (ICSD 15167) and $Sr(OH)_2.H_2O$ (ICSD 63016). They presented 15% of cubic $CoFe_2O_4$, 33% of $Sr(OH)_2.H_2O$, and 52% of $Sr(OH)_2$. Hence, there was no crystalline phase changing of the $CoFe_2O_4$ NPs, and the hydroxide phase of strontium prevailed in the synthesis process since the transformation of the SrO (produced by the calcination) in $Sr(OH)_2$ is fast under room conditions.[32] Then, the modified magnetic support was designated: $Sr(OH)_2/CoFe_2O_4$. The confirmation of the $Sr(OH)_2$ sites on the $CoFe_2O_4$ NPs surface was obtained by elemental composition analysis using mapping in STEM mode. Figure 2a shows the spectrum image scanning of $Sr(OH)_2/CoFe_2O_4$ support, and Figures 2b-2e illustrate the STEM-EDS images for the as-synthesized support. Thus, the elemental mapping shows Fe and Co distributed all over the material once the $CoFe_2O_4$ NPs were the material of immobilization, while the wide distribution of Sr and O settles the good interaction between the materials.

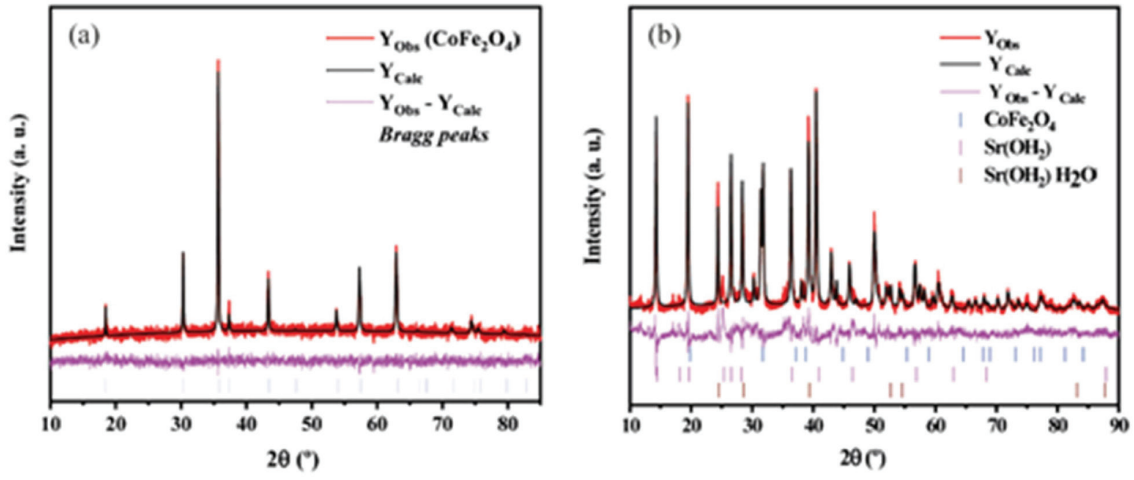

Figure 1. Rietveld refinement plot for (a) $CoFe_2O_4$ NPs and (b) $Sr(OH)_2/CoFe_2O_4$ support, presenting the observed, calculated, and difference of X-ray patterns.

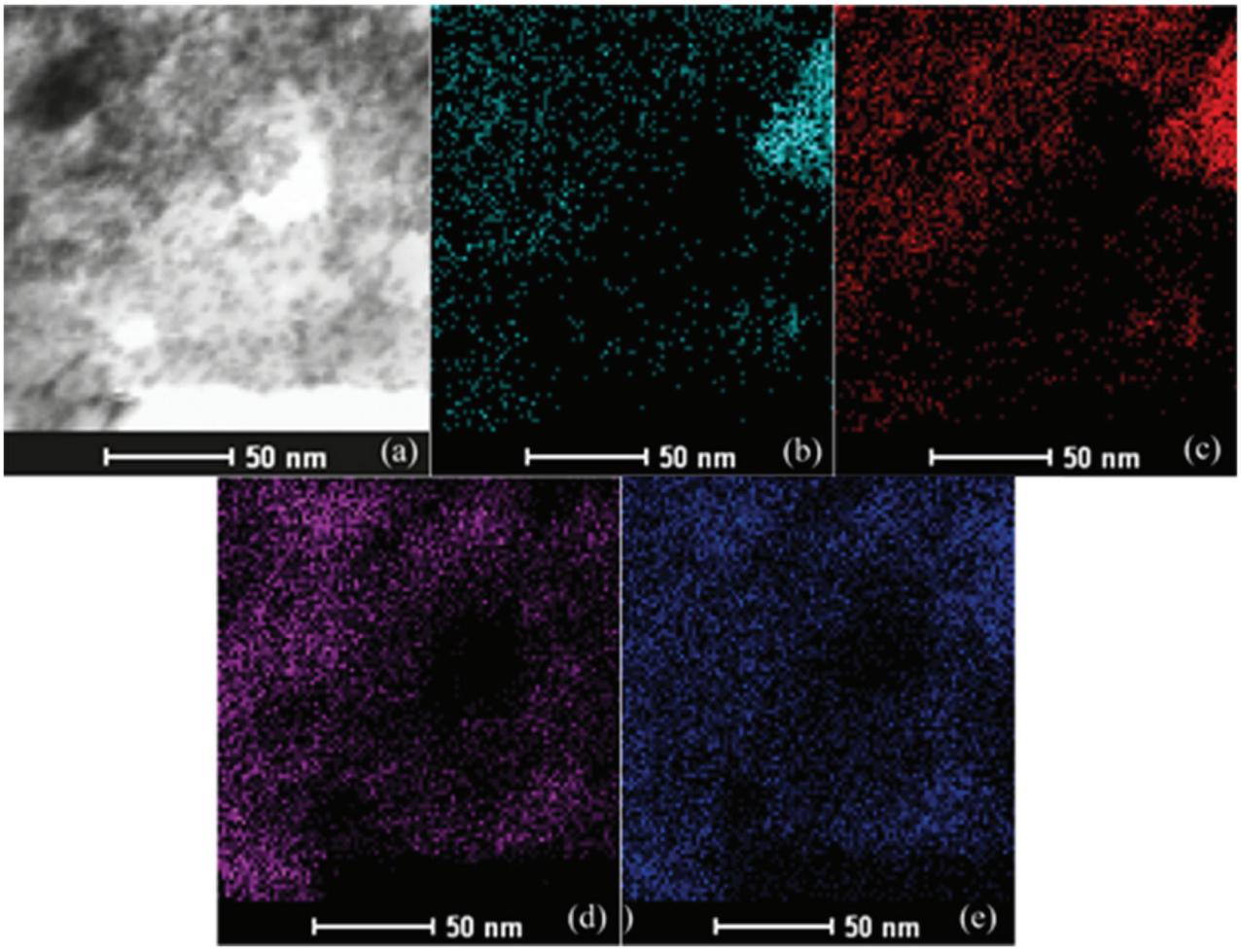

Figure 2. The morphology of the as-prepared support in the (a) spectrum image scanning and the STEM-EDS images of (b) Co, (c) Fe, (d) Sr, and (e) O.

Evaluation of the support effect on the oxidation of benzyl alcohol

As a model reaction, benzyl alcohol is suitable for the purposes of the studies herein presented. The possible products for the oxidation of benzyl alcohol are shown in Scheme 1. Although other products can be formed, it is important to establish that the main products obtained during our studies were: benzaldehyde, benzyl benzoate, and benzoic acid (except when mentioned).

Before the evaluation of the effect of the support in the oxidation, a blank reaction was carried out without catalyst or support, as shown in Figure 3a. The solvent-less reaction conditions were: 100 °C, 2 bar of O_2, and 9.6 mmol of benzyl alcohol. Although such a feature is neglected, the oxidation of benzyl alcohol without active species, i.e., Au and Pd (for our proposes), may be very important to discuss any support effect on the system.

The blank reaction presented a significant conversion, reaching 47% of conversion after 210 min, with 45% of selectivity for benzaldehyde, 30% of benzoic acid, and

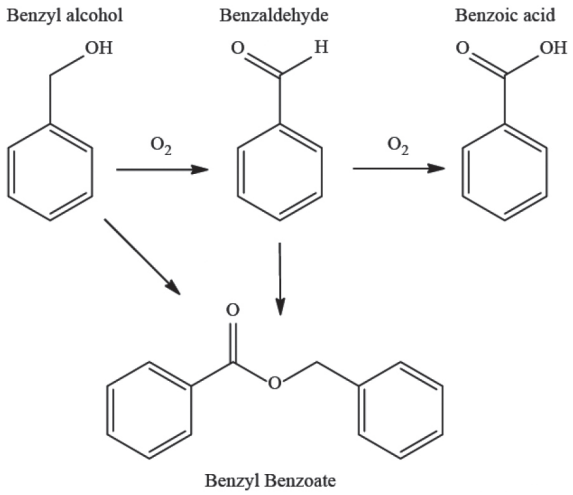

Scheme 1. Products obtained from the benzyl alcohol oxidation during the studies herein performed.

25% for benzyl benzoate. Mostly, we have observed that the benzaldehyde kept its selectivity. However, it is interesting to observe, in the time online profile presented for the blank reaction (Figure 3a), the increase in the

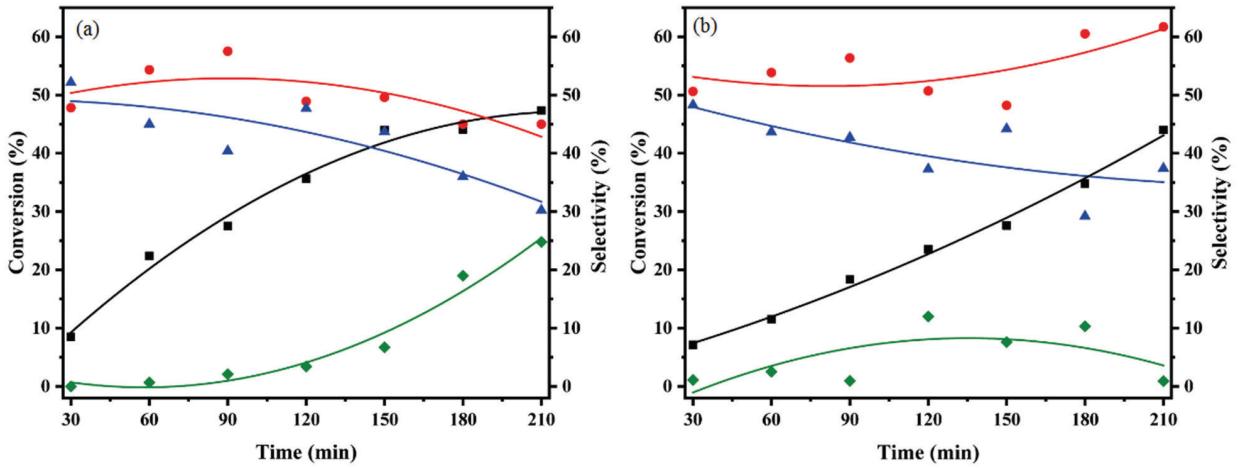

Figure 3. Time online profiles for (a) the oxidation of benzyl alcohol without support or active species and (b) catalytic oxidation of benzyl alcohol with the support. Reaction conditions: 100 °C, 2 bar of O_2, and 9.6 mmol of benzyl alcohol; solvent-less. (■) Conversion; (●) benzaldehyde; (▲) benzoic acid; (◆) benzyl benzoate.

benzyl benzoate formation, which can be produced from benzaldehyde, which is oxidized to benzyl benzoate in the presence of benzyl alcohol. The comparison of Figures 3a and 3b shows that the reaction with the support presented a lower conversion than the previous blank reaction, particularly in the first 2.5 h. Accordingly to time online profile, the formation of benzyl benzoate was very low during all the time of the reaction (210 min), presenting an improvement for the benzaldehyde (62%) formation, keeping the benzoic acid production lower (37%) than in the blank reaction.

According to the Figure 3, the conversion after 210 min for the blank test was 47%, and in the presence of support was 44%. The selectivity yield leads to ca. 21% *versus* 29% of benzaldehyde, and ca. 14% *versus* 17% of benzoic acid for blank test and the test with support, respectively. In catalysis, it can be considered the same considering an error of at least 5%. Only the yield of benzyl benzoate was higher for the test with support owing to the basic features. The literature[36-39] have dealt with many examples of catalytic supports that have no activity by itself or with gold NPs on it without external base addition; thus, it can be an interesting feature for oxidation reaction of other substrates, although any substantial effect of the support itself was not identified.

Catalyst syntheses and Au:Pd ratio effect

Supported gold-palladium NPs are important once they are well known as active catalysts for alcohol oxidation without the necessity of an external base addition;[40,41] associating these NPs with the modified-magnetic support, the system could reach an improved performance. Thus, catalysts were prepared as mono- and bimetallic counterparts, one can assume that the use of monometallic catalysts is essential to study the bimetallic effect, always maintaining 2% of loading in all the catalysts (confirmed by FAAS). PVA-stabilized NPs were prepared by reduction with $NaBH_4$ as this colloidal route promotes the preparation of relatively monodisperse particles. As an initial screening, the NPs were prepared using the following ratios: Au:Pd 1:0 (100 mol% Au), AuPd 1:1 (50 mol% Au:50 mol% Pd), AuPd 1:1.5 (40 mol% Au:60 mol% Pd), AuPd 1:2 (33 mol% Au:67 mol% Pd), Au:Pd 0:1 (100 mol% Pd). After the syntheses, the NPs were impregnated on the $Sr(OH)_2/CoFe_2O_4$ support and designated as AuPd(X:Y)/$Sr(OH)_2/CoFe_2O_4$ catalysts, where X:Y indicated the nominal Au:Pd ratios. Important to state that other Au:Pd ratios, with an increased Pd quantity, were not possible to be synthesized; it seems that the NPs synthesis protocol used herein does not stand increased amounts of Pd when Au ions are present in the system.

The as-prepared materials were submitted to FAAS and XPS techniques to guarantee the ratios nominally considered (Table 1). Noticeably, the results are in a close agreement with the nominal determined synthesis, and the FAAS ratio and Au and Pd at.% are also very aligned with each other.

Focusing on the materials comprised of AuPd NPs, which is the aim of the studies, TEM images were used to analyze the metal NPs size and morphology. An important feature targeted herein was the obtaining of $CoFe_2O_4$ NPs exposing $Sr(OH)_2$ spots that would provide sites for the NPs immobilization, obtaining an advantage from their effect on the catalysis, as well as their interaction with the metals. As a typical characteristic of the three materials, the aimed synthesis was achieved (Figure S1, Supplementary Information (SI) section). The images and

Table 1. Pd:Au ratio and metal exposure for monometallic and bimetallic catalysts

Catalyst	Pd:Au ratio		Au / at.%	Pd / at.%
	AAS	XPS		
$Au(1:0)/Sr(OH)_2/CoFe_2O_4$	–	–	2.90	–
$AuPd(1:1)/Sr(OH)_2/CoFe_2O_4$	1.10	1.05	6.11	6.44
$AuPd(1:1.5)/Sr(OH)_2/CoFe_2O_4$	1.45	1.54	5.57	8.57
$AuPd(1:2)/Sr(OH)_2/CoFe_2O_4$	1.85	1.60	8.74	13.90
$Pd(0:1)/Sr(OH)_2/CoFe_2O_4$	–	–	–	3.76

AAS: atomic absorption spectroscopy; XPS: X-ray photoemission spectroscopy.

the size distribution histograms in lower magnification (Figures 4a, 4b, and 4c for the different metal ratios) revealed that the bimetallic NPs presented similar average particles sizes: $AuPd(1:1)/Sr(OH)_2/CoFe_2O_4$ (4.72 ± 3.02 nm), $AuPd(1:1.5)/Sr(OH)_2/CoFe_2O_4$ (5.34 ± 2.98 nm), $AuPd(1:2)/Sr(OH)_2/CoFe_2O_4$ (5.06 ± 2.76 nm). They presented spherical shapes, confirming that the colloidal sol prepared by using PVA

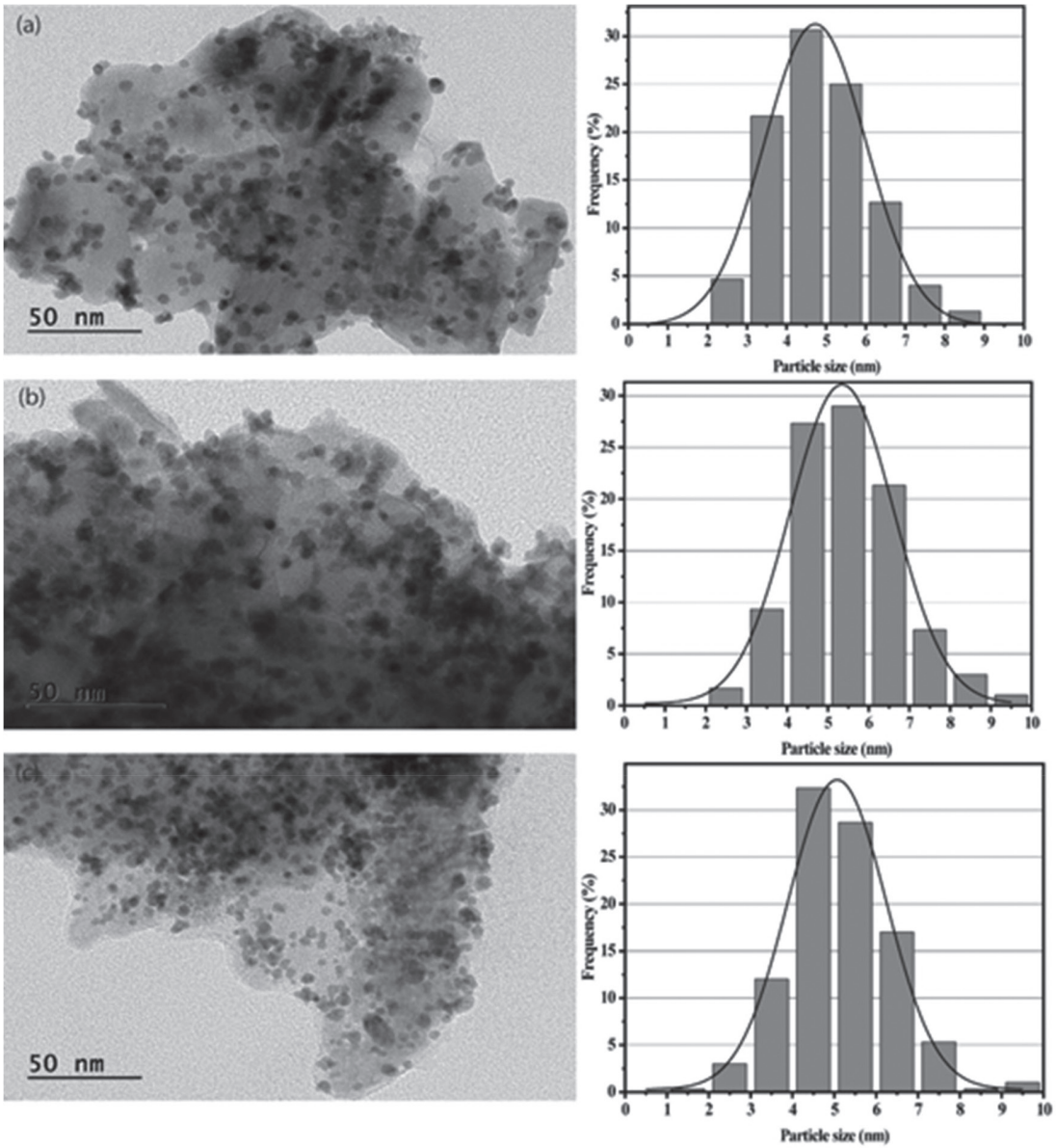

Figure 4. TEM images (left) of the (a) $AuPd(1:1)/Sr(OH)_2/CoFe_2O_4$; (b) $AuPd(1:1.5)/Sr(OH)_2/CoFe_2O_4$; and (c) $AuPd(1:2)/Sr(OH)_2/CoFe_2O_4$ catalysts and their respective size distribution histograms (right).

as a protective agent is very efficient for NPs synthesis, even with different amounts of Au and Pd. Also, the TEM images have shown a good dispersion of the AuPd NPs on the surface of the support. After the impregnation, the surface properties of the materials were analyzed (Table S1, SI section) and presented similar characteristics, possibly due to similar metal loading and particles' size.

To gain a deeper understanding of the physical features of the metal distribution, STEM-EDS elemental mapping images were attained for the three catalysts, as observed in Figure 5. Individual mappings of Au and Pd are depicted for the materials, showing that the metals distributions are overlapped with each other.

In the catalytic studies (Figure 6), using identical reaction conditions as used before, a volcano-like tendency was observed, characterized by a growth in the substrate conversion as the quantity of Pd was increased, with a decrease in the conversion for more than 60 mol% Pd. Although a slight drop was observed in the conversion of benzyl alcohol from the catalyst with 60 mol% Pd to 67 mol% Pd in 2.5 h, the selectivity improvement was remarkable, reaching 96% of benzaldehyde formation, while just 77% for this product was obtained with 60 mol% Pd catalyst, suggesting a palladium quantity effect on the NPs.

Once the TEM and STEM-EDS elemental mapping were not sufficient for explaining the performance

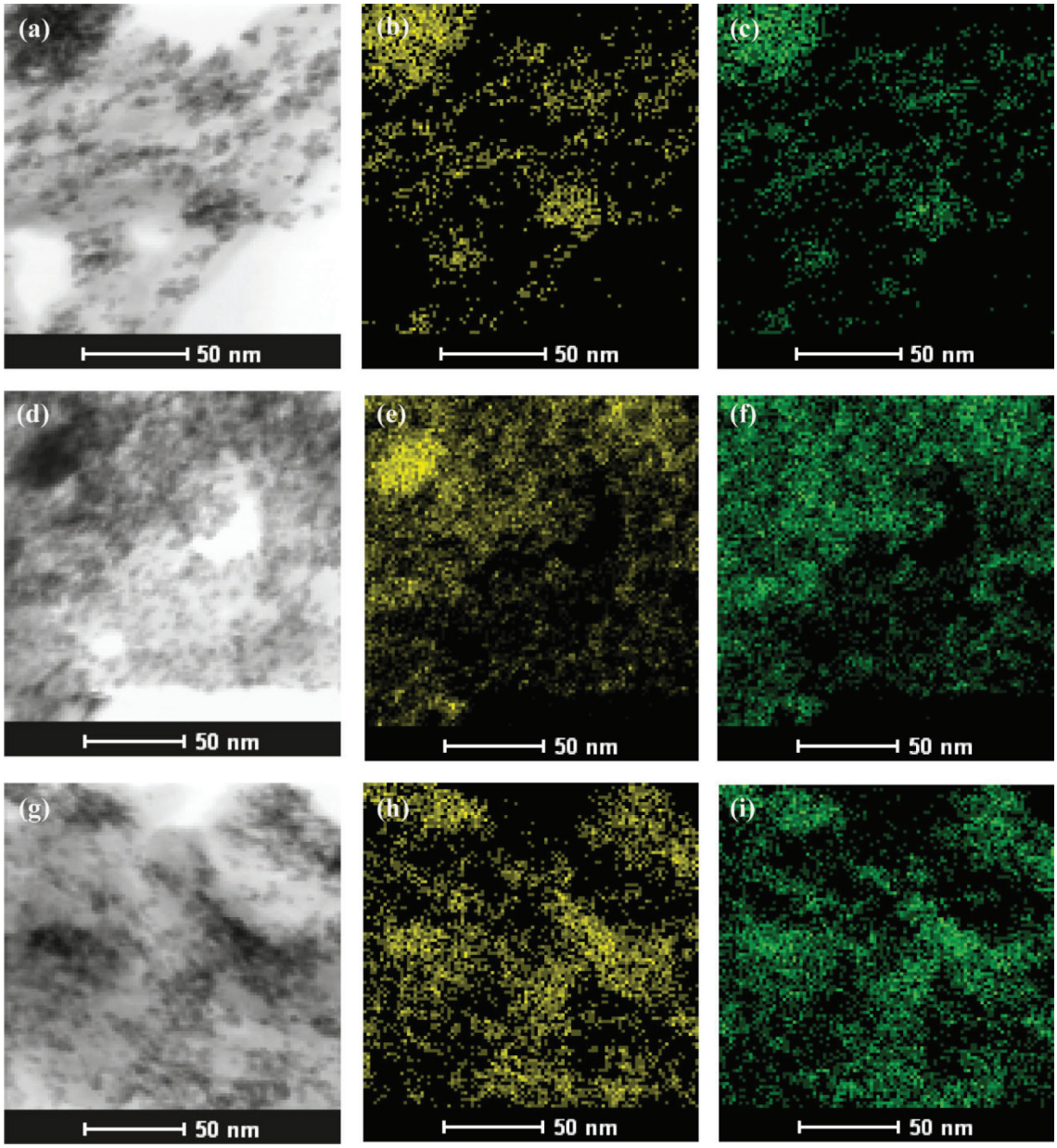

Figure 5. Morphology of the (a) AuPd(1:1)/$Sr(OH)_2$/$CoFe_2O_4$; (d) AuPd(1:1.5)/$Sr(OH)_2$/$CoFe_2O_4$; (g) AuPd(1:2)/$Sr(OH)_2$/$CoFe_2O_4$ catalysts in the spectrum image scanning. STEM-EDS elemental map images of (b, e, h) Au and (c, f, i) Pd.

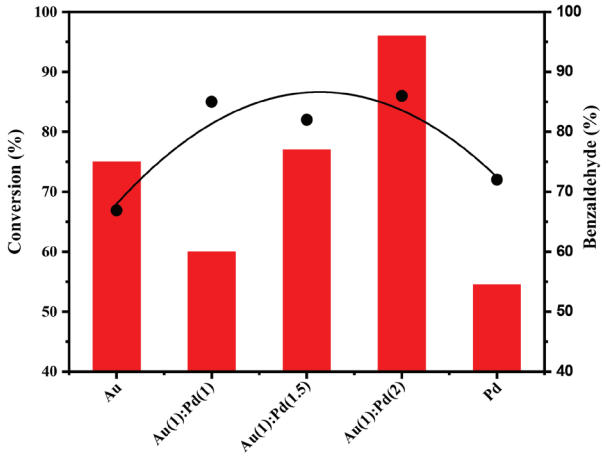

Figure 6. Catalytic performance of the catalysts in the oxidation of benzyl alcohol. Reaction conditions: 100 °C, 2.5 h, 2 bar of O_2, and 9.6 mmol of benzyl alcohol; solvent-less. To facilitate the viewing, just the Au:Pd molar ratio was included in the figure.

differences among the catalyst, XPS was employed again, using the values of binding energy (BE) for the Au 4f and Pd 3d regions (Figure 7). Starting with the XPS of Pd 3d spectra, the peaks at 334.8 and 340.9 eV are assigned to Pd^0 species in the monometallic catalyst $Pd/Sr(OH)_2/CoFe_2O_4$. However, the bimetallic materials presented Pd 3d spectra that were possible to be deconvoluted into four peaks, presenting oxidized species: $AuPd(1:1)/Sr(OH)_2/CoFe_2O_4$ (Pd^0 = 334.6 and 339.7 eV; Pd^{2+} = 336.8 and 341.6 eV); $AuPd(1:1.5)/Sr(OH)_2/CoFe_2O_4$ (Pd^0 = 334.5 and 339.7 eV; Pd^{2+} = 335.9 and 341.5 eV); $AuPd(1:2)/Sr(OH)_2/CoFe_2O_4$ (Pd^0 = 334.2 and 339.7 eV; Pd^{2+} = 335.7 and 341.6 eV).

In the Au 4f spectra, one can notice that the spectra for the monometallic catalyst ($Au/Sr(OH)_2/CoFe_2O_4$) present only two peaks (Au $4f_{7/2}$ = 82.7 and Au $4f_{5/2}$ = 86.4), which are assigned to Au^0 species. However, as observed for the Pd spectra, oxidized Au species also were observed. For the $AuPd(1:1)/Sr(OH)_2/CoFe_2O_4$ catalyst, the peaks located at 83.0 and 86.6 are related to Au^0 species, while the peaks located at 84.3 and 87.8 eV are related to $Au^{\delta+}$ species. For the $AuPd(1:1.5)/Sr(OH)_2/CoFe_2O_4$ catalyst, the peaks centered at values of BE of 82.7 and 86.4 eV are assigned to Au^0 species, and the peaks at BE of 83.8 and 87.4 eV are related to cationic gold species. The $AuPd(1:2)/Sr(OH)_2/CoFe_2O_4$ catalyst presents two peaks for Au^0 species (82.5 and 86.2 eV) and two peaks for $Au^{\delta+}$ species (83.6 and 87.3 eV). The values of BE shift gradually to lower energies for the Au XPS peaks as the Pd content increases, while the Pd spectra present shifts only for the peaks of $Pd3d_{5/2}$. The shifts in values of BE for Au spectra indicate changes in the electronic properties of the metal; the same can be associated with the peaks of Pd $3d_{5/2}$. However, only one peak of the Pd spectra presents such a feature; thus, the XPS data, associated with the elemental mapping, indicate a close position of the metals and contact with them, without necessarily the formation of an alloy.

The gold species on the surface of the materials presented remarkable differences (Table S2, SI section). When the Au:Pd 1:1 NPs were impregnated onto the support, the major gold species on the surface of the catalyst is metallic (83.3%), with a minor contribution of the positively charged $Au^{\delta+}$ species (16.7%). A significant difference was observed for the $AuPd(1:1.5)/Sr(OH)_2/CoFe_2O_4$, with 41.3% of Au^0 and 58.7% of $Au^{\delta+}$. Interestingly, the $AuPd(1:2)/Sr(OH)_2/CoFe_2O_4$ catalyst presented similar quantities of both species (52.9% for Au^0 and 48.1% for $Au^{\delta+}$).

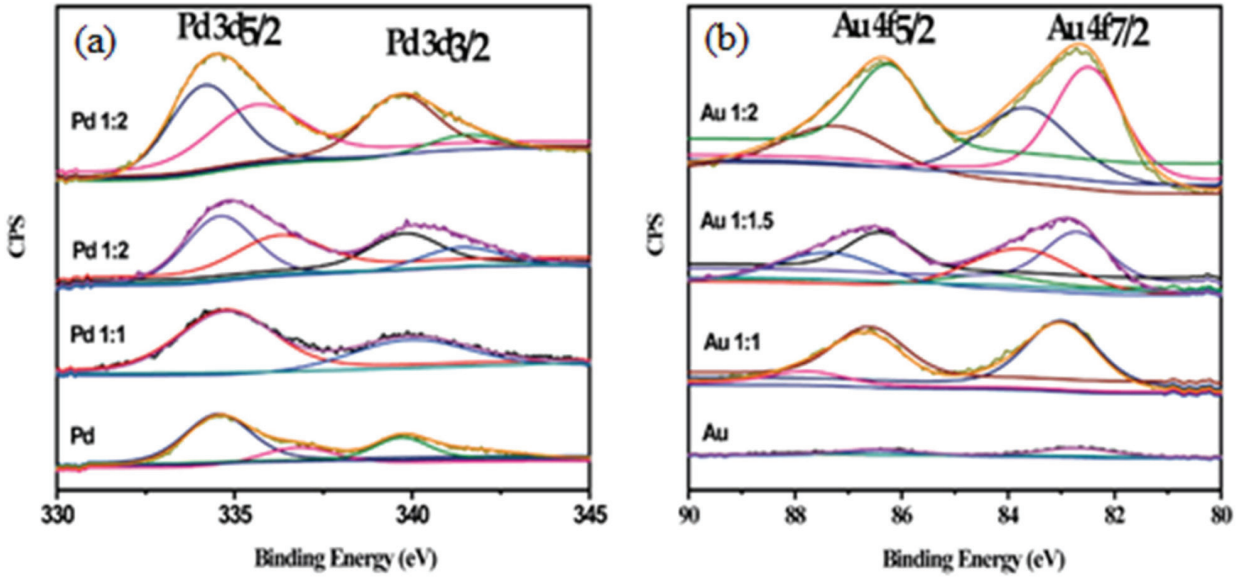

Figure 7. XPS spectra of Au:Pd varying the molar ratio of Au to Pd. (a) Pd 3d and (b) Au 4f regions.

The interaction among Au, Pd, and the support induce speciation changes on the system. We have published[35] before a catalyst using Au:Pd 1:1.5 NPs supported on $SrCO_3$, which presented NPs with just metallic species for both metals; thus, the data presented herein suggest that the support has some effect on the NPs species during the impregnation step, in addition to the effect that Au and Pd atoms have over each other.

Possessing all the information showed, two main characteristics seem to govern the activity and selectivity of the systems: the Pd amount and the Au species quantities. It is clear that the increase on the Pd amount promotes a performance improvement; however, the data on Table 1 shows that the Pd:Au ratio determined by XPS is similar to the catalysts AuPd(1:1.5)/$Sr(OH)_2$/$CoFe_2O_4$ and AuPd(1:2)/$Sr(OH)_2$/$CoFe_2O_4$. Therefore, the metal ratio calculated by XPS on both is similar, while the gold species are very different (Table 1), which leads us to believe that similar quantities of metallic and positively charged species of gold are the most important feature for the performance changes. In addition, such systems comprised of Au and Pd are believed to be more active due to charge transfer between Pd and Au, indicating that the electronic structure of the surface Au atoms was modified upon the addition of Pd. This feature highly affects the performance of a bimetallic catalyst when compared to its monometallic counterpart.

Analyzing the time online profile (Figure 8a) for the catalysts, including the reaction with the support for comparison, it is easy to observe that the activity of the systems is quite linear during the progress of the reaction. In addition, the activity of the AuPd(1:1.5)/$Sr(OH)_2$/$CoFe_2O_4$ and AuPd(1:2)/$Sr(OH)_2$/$CoFe_2O_4$ catalysts is similar. The initial low selectivity for the three catalysts follows the stated before, which we reasoned by a low quantity of benzaldehyde in the reaction medium; however, the system comprised of Au:Pd 1:1 does not reach an

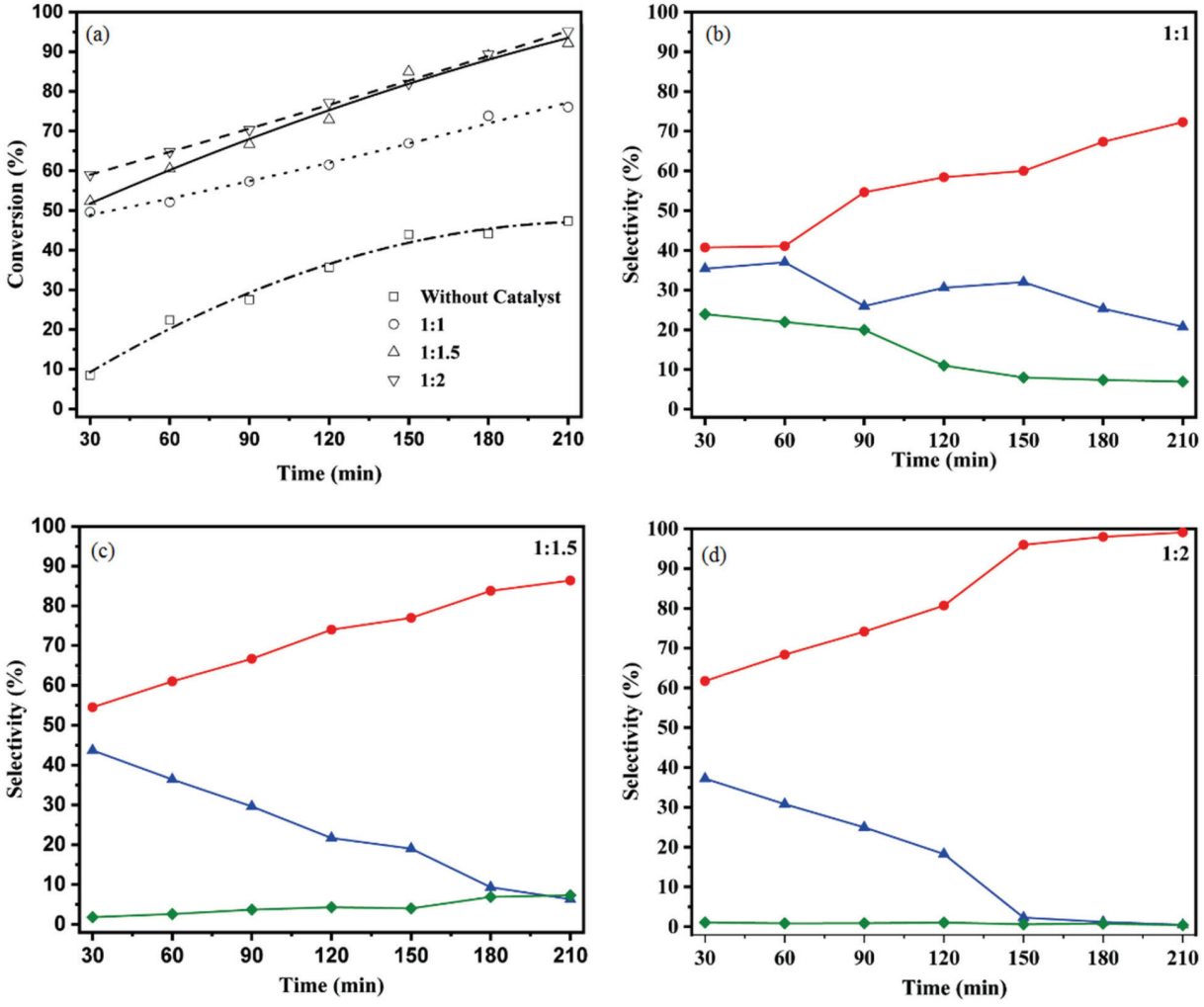

Figure 8. Time online profiles for (a) conversion of the three catalysts and support; selectivity of the (b) AuPd(1:1)/$Sr(OH)_2$/$CoFe_2O_4$; (c) AuPd(1:1.5)/$Sr(OH)_2$/$CoFe_2O_4$; (d) AuPd(1:2)/$Sr(OH)_2$/$CoFe_2O_4$ catalysts. Reaction conditions: 100 °C, 2 bar of O_2, 9.6 mmol of benzyl alcohol; solvent-less. Selectivity for (●) benzaldehyde; (▲) benzoic acid; (◆) benzyl benzoate.

acceptable selectivity, different from the other two catalysts. After 3.5 h, the AuPd(1:2)/$Sr(OH)_2$/$CoFe_2O_4$ catalyst reaches > 99% of selectivity for benzaldehyde, which is an incredible result. However, the AuPd(1:1.5)/$Sr(OH)_2$/$CoFe_2O_4$ catalyst also reaches a good selectivity, presenting 86% of benzaldehyde after 3.5 h. However, the carbon balance of the systems are quite compromised after the reaction completion for the three cases once the Pd-based catalysts favor the decarboxylation of benzoic acid.

The optimization of the reaction conditions for the Au:Pd 1:1.5 system would provide important information on the previous inferences regarding the performance of the catalysts. It would attest to the necessity of having such quantities of gold and palladium species for the selectivity.

Optimizing the oxidation of benzyl alcohol using the AuPd(1:1.5)/$Sr(OH)_2$/$CoFe_2O_4$ catalyst

Experimental conditions were analyzed to improve the catalyst performance of the AuPd(1:1.5)/$Sr(OH)_2$/$CoFe_2O_4$ catalyst. Table 2 shows the temperature effect on the activity and selectivity of the material. Maintaining the pressure of the system in 2 bar, it can be noticed that the temperature increasing, from 80 to 120 °C (entries 1-5), promotes conversion improvement, which goes from 52 to 94%. Also, an enhancement on the selectivity to benzaldehyde was observed (88% in 2.5 h, while the Au:Pd 1:2 system reached 96% in the same period). Any increase in the temperature above 120 °C could have damaged the glass Fisher-Porter reactor, or makes it dangerous. Thus, considering the reaction apparatus used in the studies, the temperature was not sufficient to reach the same selectivity of the AuPd(1:2)/$Sr(OH)_2$/$CoFe_2O_4$ catalyst. Maintaining the temperature at 120 °C, the pressure of the system was modified from 1 to 4 bar (entries 6-9, Table 3). Interestingly, the pressure has some effect on the conversion, but not on the selectivity improvement, causing more benzyl benzoate formation with the pressure augmentation. It seems that the selectivity does not present a kinetic regime but rather an electronic issue, corroborating the detailed findings presented before.

Effect of oxygen content, water, and mechanistic considerations

The role of oxygen in the oxidation of alcohol is still under discussion, so that is important to bring some sights regarding its effect in the studied system. Recently, Hutching and co-workers[42] have published the effect of water and O_2 in the oxidation of cinnamaldehyde alcohol. Interestingly, they have shown that an AuPd/TiO_2 catalyst, prepared in conditions similar to those used here, presented a remarkable activity (86%) under anaerobic conditions. They have proposed that the hydrogen is abstracted on the catalyst surface, which is in agreement with the proposed mechanisms for AuPd-promoted benzyl alcohol oxidations, and the reaction suffers hydrogenation/hydrogenolysis. Although the reaction pathways are different for each substrate, we decide to guarantee the effect of O_2 in the system.

Table 2. Catalytic evaluation of the benzyl alcohol oxidation using the AuPd(1:1.5)/$Sr(OH)_2$/$CoFe_2O_4$ catalyst with different temperatures[a]

entry	Temperature / °C	Conversion / %	Selectivity / %		
			Benzaldehyde	Benzoic acid	Benzyl benzoate
1	80	52	64	32	4
2	90	76	70	26	4
3	100	85	77	19	4
4	110	93	79	11	10
5	120	94	88	2	10

[a]Reaction conditions: 9.6 mmol of benzyl alcohol, Au:Pd molar ratio of 1:1.5, 2 bar of O_2, 2.5 h.

Table 3. Catalytic evaluation of the benzyl alcohol oxidation using the AuPd(1:1.5)/$Sr(OH)_2$/$CoFe_2O_4$ catalyst with different pressures[a]

entry	Pressure / bar	Conversion / %	Selectivity / %		
			Benzaldehyde	Benzoic acid	Benzyl benzoate
6	1	85	81	15	4
7	2	94	88	2	10
8	3	94	76	3	21
9	4	96	62	4	34

[a]Reaction conditions: 9.6 mmol of benzyl alcohol, Au:Pd molar ratio of 1:1.5, reaction temperature 120 °C, 2.5 h.

Table 4. Catalytic evaluation of the benzyl alcohol oxidation using the AuPd(1:2)/$Sr(OH)_2$/$CoFe_2O_4$ catalyst[a]

entry	Condition	Conversion / %	Selectivity / %		
			Benzaldehyde	Benzoic acid	Benzyl benzoate
10	blank, N_2[b]	1.0	99	–	1
11	catalyst, N_2[b]	1.0	100	–	–
12	blank, N_2[b] + water[c]	1.4	100	–	–
13	catalyst, N_2[b] + water[c]	1.0	100	–	–
14	blank, O_2[b] + water[c]	1.0	100	–	–
15	catalyst, O_2[b] + water[c]	7.6	91	9	–

[a]Reaction conditions: 9.6 mmol of benzyl alcohol, 120 °C, 2.5 h; [b]2 bar of gas (O_2 or N_2); [c]0.5 mL of water.

The blank and the AuPd(1:2)/$Sr(OH)_2$/$CoFe_2O_4$ catalyzed reactions, under N_2 pressure, with or without water, did not present any activity once the data presented in entries 10-13 (Table 4) are the same observed for the basal substrate, without reaction. The same reactions (catalyzed and not catalyzed) underwent the same reaction, switching the N_2 for O_2 with water addition; again, the blank reaction under these conditions did not present any activity (entry 14). The catalyzed reaction presented a conversion of 7.6% and followed the same trend as before: benzoic acid formation at the beginning.

Thus, the reaction is just possible to proceed using an oxygen donor; in the present case, the molecular oxygen. However, the water content decreased the catalyzed reaction significantly and quenched the reaction to occur in the black reaction. We reasoned that these findings are due to the lower oxygen solubility in water when compared to the solvent-less reactions. Also, water can be effective in segregating the radicals, acting as hydrogen-bonded to the radicals.[43] Another possibility may be the interaction of water with basic sites, either by blocking them or by dissolving the $Sr(OH)_2$ impregnated.

Based on the above considerations, a mechanism proposal is shown in Figure 9 in an attempt to explain the prominent selectivity of the AuPd(1:2)/$Sr(OH)_2$/$CoFe_2O_4$ catalyst. The presence of NPs in the bimetallic Au:Pd 1:2 ratio enhanced the activity of the oxidation reaction and changed aspects of the reaction pathway, as discussed before. In a first step, the higher electronegativity of Au attracts electrons from Pd, causing O_2 activation by electrons from the NPs surface (I). As discussed before, the support may cause abstraction of the proton from the substrate, intercept radicals (alkoxide intermediates), and transfer them to the NPs surface (II), although it might also happen on the NPs surface. The intermediate forms an unstable metal-alcoholate (III), which undergoes a β-hydride elimination, with the release of benzaldehyde. The oxygen species remove H from the NPs surface with H_2O elimination, restoring the catalyst for a new cycle.

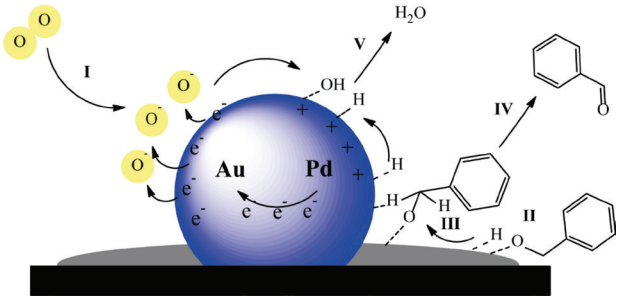

Figure 9. Proposed reaction pathway for the solvent-free oxidation of benzyl alcohol over AuPd(1:2)/$Sr(OH)_2$/$CoFe_2O_4$ catalyst for benzaldehyde formation.

Such mechanism matches to all the observations before: the necessity of having benzyl alcohol and benzaldehyde in the medium for the inhibition of benzoic acid formation and a specific Au:Pd ratio. The proposed mechanism is considered after the above requirements are filled.

Catalyst stability

An important feature of a catalytic system is its recyclability. Although the remarkable performance of a material is highly desired, heterogeneous catalysts, in special the magnetic ones, are designed to be used several times. As shown in Figure 10, the AuPd(1:2)/$Sr(OH)_2$/$CoFe_2O_4$ catalyst maintained its conversion in five cycles without loss of activity. Most notably, its selectivity kept nearly unchanged after the five runs. Tests of leaching were performed by FAAS and confirmed that the material kept its metal loading after the recycling experiments. Thus, the material presents the potential to be used in further runs.

Conclusions

In the studies herein presented, we have proposed the synthesis of a magnetic-modified support, comprised of $Sr(OH)_2$ and $CoFe_2O_4$ NPs, for the oxidation of benzyl alcohol. After the immobilization of AuPd NPs in different ratios on the prepared magnetic material, we systematically

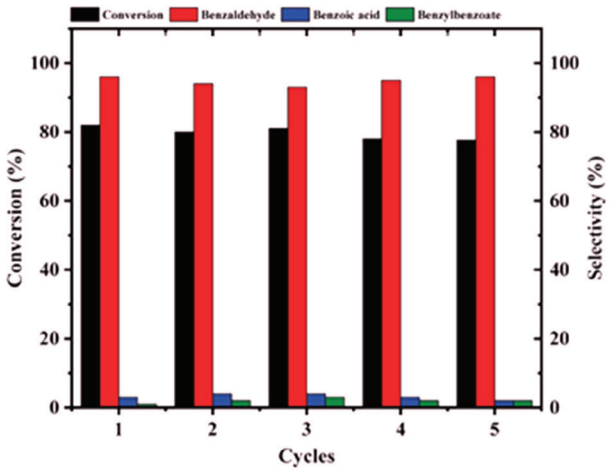

Figure 10. Recycling tests for the AuPd(1:2)/$Sr(OH)_2$/$CoFe_2O_4$ catalyst in benzyl alcohol oxidation. Reaction conditions: 100 °C, 2.5 h, 2 bar of O_2, 9.6 mmol of benzyl alcohol; solvent-less.

studied by XPS and catalytic essays the origin of different performances regarding the quantity of palladium and gold species. Also, the association of XPS, TEM, and STEM-EDS images were able to characterize the catalyst fully.

Optimization tests were capable of corroborating our proposition about the basis of the NPs effects on the performance of the catalyst, demonstrating that a judicious choice of the ratio of the metals prevents the necessity of manipulating the reaction conditions to improve the performance of the system. Studies under N_2 and O_2 environments, with or without water, confirmed the role of the O_2 in the system; this finding allowed us to propose a mechanism for the novel catalyst. Also, the catalyst was stable up to five runs without loss of activity or selectivity.

Supplementary Information

Supplementary data with the EDS spectra of the AuPd (1:1)/$Sr(OH)_2$/$CoFe_2O_4$ catalyst, surface properties of the catalysts, and information on surface metal compositions revealed by XPS analysis, are available free of charge at http://jbcs.sbq.org.br as PDF file.

Acknowledgments

The authors acknowledge financial support from Capes and CNPq. The authors also acknowledge Dr Liane M. Rossi for the atomic absorption analyses. The authors thank to CCMC/CDMF (FAPESP No. 2013/07296-2, Brazil) for the XPS measurements.

Author Contributions

Laíse N. S. Pereira was responsible for the data curation, investigation, visualization, writing original draft, review and editing; Marco A. S. Garcia for the conceptualization, writing original draft, review and editing; Jennifer Rozendo for the investigation; Pedro Vidinha for the resources, supervision, writing review and editing; Alfredo Duarte for the data curation; Carla V. R. de Moura for the visualization; Edmilson M. de Moura for the conceptualization, funding acquisition, resources and validation.

References

1. Khawaji, M.; Chadwick, D.; *ChemCatChem* **2017**, *9*, 4353.
2. Tsuchiya, D.; Tabata, M.; Moriyama, K.; *Tetrahedron* **2012**, *68*, 6849.
3. Sigman, M. S.; Jensen, D. R.; *Acc. Chem. Res.* **2006**, *39*, 221.
4. Valange, S.; Védrine, J. C.; *Catalysts* **2018**, *8*, 483.
5. Zha, G.; Fang, W.; Leng, J.; Qin, H.; *Adv. Synth. Catal.* **2019**, *361*, 2262.
6. Muzart, J.; *Chem. Rev.* **1992**, *92*, 113.
7. Wallace, T. J.; *J. Org. Chem.* **1959**, *24*, 1051.
8. Porta, F.; Prati, L.; Rossi, M.; Coluccia, S.; Martra, G.; *Catal. Today* **2000**, *61*, 165.
9. Prati, L.; Rossi, M.; *J. Catal.* **1998**, *176*, 552.
10. Prati, L.; Martra, G.; *Gold Bull.* **1999**, *32*, 96.
11. Ferraz, C. P.; Garcia, M. A. S.; Teixeira-Neto, É.; Rossi, L. M.; *RSC Adv.* **2016**, *6*, 25279.
12. Haruta, M.; *Faraday Discuss.* **2011**, *152*, 11.
13. Gómez-Villarraga, F.; Radnik, J.; Martin, A.; Köckritz, A.; *J. Nanopart. Res.* **2016**, *18*, 141.
14. Wang, A.; Yan, X.; Mou, C.; Zhang, T.; *J. Catal.* **2013**, *308*, 258.
15. Zhu, X.; Guo, Q.; Sun, Y.; Chen, S.; Wang, J.-Q.; Wu, M.; Fu, W.; Tang, Y.; Duan, X.; Chen, D.; Wan, Y.; *Nat. Commun.* **2019**, *10*, 1428.
16. Grunwaldt, J.; Caravati, M.; Baiker, A.; *J. Phys. Chem.* **2006**, *110*, 25586.
17. Hardacre, C.; Mullan, E. A.; Rooney, D. W.; Thompson, J. P.; *J. Catal.* **2005**, *232*, 355.
18. Ma, T.; Liang, F.; Liu, R.; Zhang, H.; *Nanomaterials* **2017**, *7*, 239.
19. Villa, A.; Wang, D.; Su, D. S.; Prati, L.; *Catal. Sci. Technol.* **2015**, *5*, 55.
20. Pan, Y.; Shen, X.; Yao, L.; Bentalib, A.; Peng, Z.; *Catalysts* **2018**, *8*, 2.
21. Corma, A.; Iborra, S.; *Adv. Catal.* **2006**, *49*, 239.
22. Zhang, G.; Hattori, H.; Tanabe, K.; *Appl. Catal.* **1988**, *36*, 189.
23. Rossi, L. M.; Costa, N. J. S.; Silva, F. P.; Wojcieszak, R.; *Green Chem.* **2014**, *16*, 2906.
24. Liu, X.; Conte, M.; *Phys. Chem. Chem. Phys.* **2014**, *17*, 715.
25. Sankar, M.; Nowicka, E.; Carter, E.; Murphy, D. M.; Knight, D. W.; Bethell, D.; Hutchings, G. J.; *Nat. Commun.* **2014**, *5*, 3332.

26. Jagminas, A.; Kurtinaitienė, M.; Mažeika, K.; *Chemija* **2013**, *24*, 103.
27. Hu, S.; Guan, Y.; Wang, Y.; Han, H.; *Appl. Energy* **2011**, *88*, 2685.
28. de Moura, E. M.; Garcia, M. A. S.; Gonçalves, R. V.; Kiyohara, P. K.; Jardim, R. F.; Rossi, L. M.; *RSC Adv.* **2015**, *5*, 15035.
29. Bortolotti, M.; Lutterotti, L.; Lonardelli, I.; *J. Appl. Crystallogr.* **2009**, *42*, 538.
30. *CasaXPS Processing Software*, version 2.3.15; Casa Software Ltd., Teignmouth, UK, 2018.
31. *ImageJ*, 1.52v; Laboratory for Optical and Computational Instrumentation (LOCI), University of Wisconsin, USA, 2012.
32. Castro, K. P. R.; Garcia, M. A. S.; de Abreu, W. C.; de Sousa, A. A.; de Moura, C. V. R.; Costa, J. C. S.; de Moura, E. M.; *Catalysts* **2018**, *8*, 83.
33. Pereira, L. N. S.; Ribeiro, C. E. S.; Tofanello, A.; Costa, J. C. S.; de Moura, C. V. R.; Garcia, M. A. S.; de Moura, E. M.; *J. Braz. Chem. Soc.* **2019**, *30*, 1317.
34. Batista, F. S. C. L.; Melo, I. E. M. S.; Pereira, L. N. S.; Lima, A. G. P.; Bashal, A. H.; Costa, J. C. S.; Magalhães, J. L.; Lima, F. C. A.; Moura, C. V. R.; Garcia, M. A. S.; Moura, E. M.; *J. Braz. Chem. Soc.* **2020**, *31*, 488.
35. Melo, I. E. M. S.; de Sousa, S. A. A.; Pereira, L. N. S.; Oliveira, J. M.; Castro, R. P. K.; Costa, J. C. S.; de Moura, E. M.; de Moura, C. V. R.; Garcia, M. A. S.; *ChemCatChem* **2019**, *11*, 3022.
36. de Abreu, W. C.; Garcia, M. A. S.; Nicolodi, S.; de Moura, C. V. R.; de Moura, E. M.; *RSC Adv.* **2018**, *8*, 3903.
37. Klitgaard, S. K.; Dela Riva, A. T.; Helveg, S.; Werchmeister, R. M.; Christensen, C. H.; *Catal. Lett.* **2008**, *126*, 213.
38. Enache, D. I.; Knight, D. W.; Hutchings, G. J.; *Catal. Lett.* **2005**, *103*, 43.
39. Davis, R. J.; Davis, S. E.; Ide, M. S.; Davis, R. J.; *Green Chem.* **2013**, *15*, 17.
40. Silva, T. A. G.; Landers, R.; Rossi, L. M.; *Catal. Sci. Technol.* **2013**, *3*, 2993.
41. Silva, T. A. G.; Teixeira-Neto, E.; López, N.; Rossi, L. M.; *Sci. Rep.* **2014**, *4*, 5766.
42. Rucinska, E.; Miedziak, P. J.; Pattisson, S.; Brett, G. L.; Iqbal, S.; Morgan, D. J.; Sankar, M.; Hutchings, G. J.; *Catal. Sci. Technol.* **2018**, *8*, 2987.
43. Neuenschwander, U.; Hermans, I.; *J. Catal.* **2012**, *287*, 1.

Submitted: October 24, 2019
Published online: April 23, 2020